

## Colloidal Crystallization and Banding in a Cylindrical Geometry

Manouk Abkarian,<sup>†</sup> Janine Nunes,<sup>‡</sup> and Howard A. Stone<sup>\*†</sup>

*Division of Engineering and Applied Sciences, Harvard University, Cambridge, Massachusetts 02138, and  
Department of Chemistry, Morgan State University, Baltimore, Maryland 21251*

Received January 13, 2004; E-mail: has@deas.harvard.edu

Colloidal crystallization takes advantage of the strong interfacial forces<sup>1,2</sup> and tunable interactions<sup>3</sup> that organize particles into regular structures at small scales. Thus, colloidal crystallization and patterning provide a powerful and simple method to functionalize planar surfaces with monolayer and multilayer films. Applications of this self-assembly technique include the fabrication of optical,<sup>4,5</sup> catalytic,<sup>6</sup> sensing, and cleansing<sup>7</sup> materials. For example, specialized coatings of colloidal crystals on glass surfaces can lead to photonic band gap properties, which are useful in telecommunications and nonlinear optics.

Nevertheless, the ability to pattern topologically more complex surfaces such as curved, confined, or soft substrates can open new avenues for novel, “intelligent”, and responsive materials. As one step in this direction, we have performed experiments with evaporation-driven colloidal crystallization in a cylindrical configuration. In the familiar case of evaporation-driven deposition on planar substrates, colloidal crystallization occurs in the neighborhood of the contact line where the radius of curvature is necessarily of the order of magnitude of the capillary length. On the other hand, for deposition inside cylindrical capillaries, the radius of curvature is set by the radius of the capillary itself, which can be an order of magnitude or more smaller than the capillary length. In addition, confinement inside a capillary tube produces a fluid column whose length depends on the local contact angle, and this latter quantity changes if crystallization occurs at the contact line. Finally, the confinement inside the capillary also affects the evaporation rate, which can impact the kinetics of colloidal crystallization.

For the experiments reported here, the experimental setup (Figure 1) consists of a 400  $\mu\text{m}$  diameter glass capillary, held vertically in ethanol solutions of polystyrene beads (0.5  $\mu\text{m}$  in diameter). Three different initial concentrations are studied, 0.1, 0.2, and 0.4 wt %. The apparatus is maintained in an oven at 65 °C for several hours. We have conducted many other experiments, changing the particle size, the radius of the capillary tube, the concentration of the suspension, the temperature, and the solvent. The result reported here are robust and reproducible for a large range of parameters.<sup>8</sup>

In our first set of experiments, the colloids did not form a continuous film, as might have been expected on the basis of previous studies with planar substrates,<sup>4,5</sup> but rather we observed discrete bands inside the capillaries. Each band is a circular deposit of particles on the inner surface of the capillary, and the typical formation time of a single band is several minutes. The bands are shown in Figure 2 for three capillaries, each with a different initial concentration. There are two main aspects to this periodic colloidal deposit: the width and the spacing (or wavelength) of the bands generally (i) increase with the colloidal concentration and (ii) decrease in time, along the capillary, for a given initial concentration.

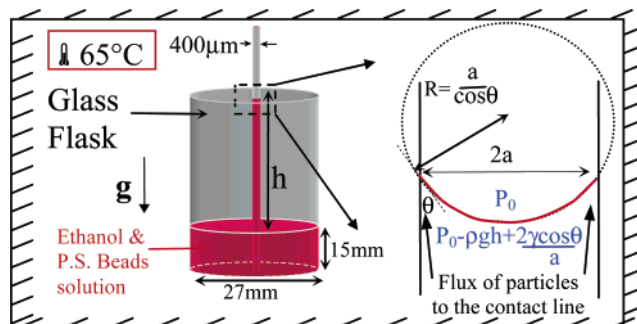


**Figure 1.** Experimental setup: a glass capillary of 400  $\mu\text{m}$  diameter is maintained vertically in an open glass bottle containing a solution of ethanol and polystyrene particles (0.5  $\mu\text{m}$  diameter). To the right, we indicate geometrical and physical parameters needed to understand the force balance in the neighborhood of the meniscus;  $\rho$  is the density and  $\gamma$  is the surface tension.

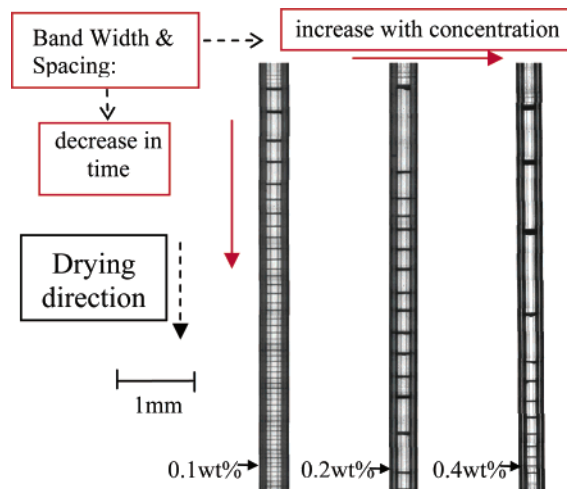


**Figure 2.** Ring patterns observed along three capillaries for three different concentrations of the particles. The black lines represent particle deposits, and the solid arrows indicate the decrease of the band width and spacing, respectively, in time and as the initial concentration increases. Each picture was produced by assembling successive microscope images of portions of the capillary.

We obtained scanning electron micrographs (SEM) of the section of the bands (along the capillary) after drying, which illustrate several significant features. As shown in Figure 3, the deposit has a smooth surface (roughness smaller than the particle size), which is asymmetric relative to the drying direction. We next focus on structural features of the colloidal deposit by providing close-up images of the leading (Figure 3c) and trailing (Figure 3d) edges. The leading edge is straight in the circumferential direction, whereas at the trailing edge there are often circumferential undulations. The height of the deposit increases smoothly from 1 layer of particles to approximately 25 layers near the middle of the band (for a typical band, not too close to the end of the drying process). The packing

<sup>†</sup> Harvard University.

<sup>‡</sup> Morgan State University.

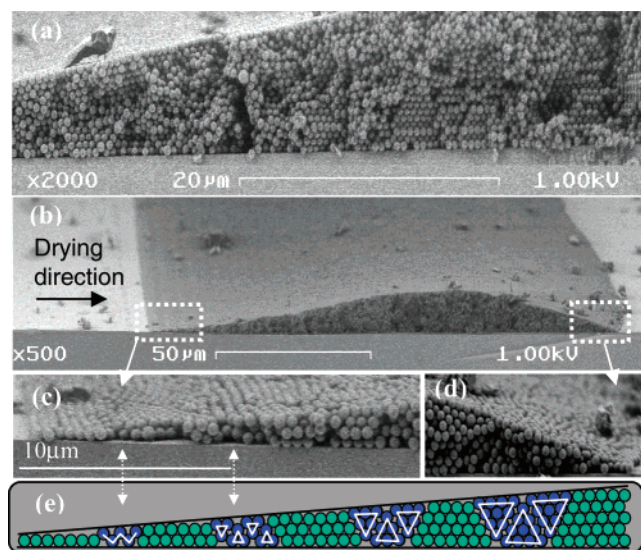


**Figure 3.** SEM pictures of a band structure in the capillary (0.2 wt % particles). (a) The top picture shows a close-up of the middle of a band, which is flat, inclined relative to the substrate, and contains closed-packed crystalline structures. (b) The middle picture shows one band, with the drying direction indicated, and the two bottom images show, respectively, on the left, (c) the smooth structure at the beginning of the band and, on the right, (d) the smooth surface at the end. (e) Schematic of the typical succession of the hexagonal close-packed regions separated by the buckled phases.

consists of a succession of hexagonally close-packed regions (both in the top view and in the thickness direction for greater than three layers), which are separated by narrow regions of “buckled phase crystals”.<sup>9</sup> The buckling refers to the transition that occurs in a confined colloidal system when the layer thickness changes by a single particle size and is indicated with white arrows in Figure 3c and 3e. In previous work,<sup>9</sup> the buckled phase was observed for suspensions confined between two parallel solid substrates, whereas here the wedge-like confinement and the successive transition in layer thickness are produced by the presence of the meniscus. Hence, during the crystallization, the system manages to maintain the highest volume fraction by forming successive hexagonal close-packed regions separated by narrow interstitial buckled regions. As a consequence, this packing leads to the smooth surfaces shown in Figure 3.

The bands are reminiscent of the sequence of irregular rings that are sometimes formed during evaporation of small droplets of a colloidal suspension.<sup>10–12</sup> Nevertheless, we note that, in the experiment reported here, the pattern formation is more regular, because of the constant radius of curvature of the meniscus throughout the evaporation process, whereas for the droplet the typical radius of curvature decreases as the volume of the droplet shrinks. In addition, the colloidal ordering at the leading edge (Figure 3c) is similar to recent studies where ordering is observed in wedges a few particles thick,<sup>13,14</sup> although we observe the large-scale (>20 particles thick) assembly shown in Figure 3.

A characteristic feature of the experiments is the formation of a nearly periodic band structure (Figure 2). A simple model for these bands, which incorporates evaporation and surface properties, may be constructed by noting that the solvent is first in contact with the glass capillary. Following convectively driven assembly of particles, the contact line is “self-pinned” by the deposition of particles and the solvent is then progressively in contact with polystyrene beads

only. The two contact angles, solvent–glass  $\theta_{SG}$  versus solvent–polystyrene  $\theta_{SP}$ , are different.<sup>15</sup> So, as the level of the fluid bath drops because of evaporation, the length  $h^{SP}$  of the column of liquid in the capillary increases relative to the surface of the fluid in the reservoir. Hence, the height of this column increases in time until the capillary forces can no longer counterbalance the gravitational force, after which the contact line slips and reaches another equilibrium position  $h^{SG}$  where the fluid is back in contact with the glass surface. Consequently, the process repeats periodically. The distance traveled by the contact line is given by  $\Delta h = h^{SG} - h^{SP} = (\gamma/\rho ga)(\cos \theta_{SG} - \cos \theta_{SP})$ ; see Figure 1. For ethanol ( $\gamma \approx 20$  mN/m) in contact successively with glass ( $\theta_{SG} \approx 5^\circ$ ) and polystyrene<sup>15</sup> ( $\theta_{SP} \approx 60^\circ$ ), we find  $\Delta h \approx 1$  mm, which is in good agreement with Figure 2 for the beginning of the band’s formation. Furthermore, we expect that the evaporation rate in the glass capillary decreases as the meniscus falls; that is, the distance to the open end of the capillary increases, which increases the length of diffusion of the vapor to the exit of the tube. Fewer particles are then deposited in time, while the rate of fall of the liquid level in the reservoir remains relatively constant. This mechanism suggests that the bands should appear narrower (Figure 2). We will compare detailed measurements with a model based upon these ideas in a future communication to explain the band width, spacing, and time variations.<sup>8</sup> We have not studied the band formation on the outside surface, which has an opposite curvature from the inner surface, but because the associated rise height is much smaller we do not expect substantial band patterning.

We believe that a better understanding of the mechanics of the band formation will allow identification of conditions for producing a continuous film of controlled shape and thickness; one step in this direction is described by Wang et al.<sup>16</sup> Such colloidal coatings in small capillaries could be used, for example, for making microfluidic devices for sensing and catalysis. In addition, capillaries with these colloidal coatings can be used to probe in a single configuration the influence of varying film thickness or a tilted surface on optical properties.

**Acknowledgment.** We thank the Harvard MRSEC for support of this research. We also thank N. D. Denkov and I. Cohen for helpful conversations, and D. Bell for technical support with the SEM pictures.

## References

- (1) Manoharan, V. N.; Elsesser, M. T.; Pine, D. *Science* **2003**, *301*, 483.
- (2) Kralchevsky, A.; Nagayama, K. *Particles at Fluid Interfaces and Membranes*; Elsevier Science: New York, 2001.
- (3) Yethiraj, A.; Van Blaaderen, A. *Nature* **2003**, *421*, 513.
- (4) Dimitrov, A. S.; Nagayama, K. *Langmuir* **1996**, *12*, 1303.
- (5) Jiang, P.; Bertone, J. F.; Hwang, K. S.; Colvin, V. L. *Chem. Mater.* **1999**, *11*, 2132.
- (6) Xia, Y.; Gates, B.; Yin, Y.; Lu, Y. *Adv. Mater.* **2000**, *12*, 693.
- (7) Wasan, D. T.; Nikolov, A. D. *Nature* **2003**, *423*, 156.
- (8) Abkarian, M.; Nunes, J.; Stone, H. A., in preparation.
- (9) Naser, S.; Bechinger, C.; Leiderer, P. *Phys. Rev. Lett.* **1997**, *79*, 2348.
- (10) Deegan, R. D.; Bakakin, O.; Dupont, T. F.; Huber, G.; Nagel, S. R.; Witten, T. A. *Nature* **1997**, *389*, 827.
- (11) Shmuylovich, L.; Shen, A. Q.; Stone, H. A. *Langmuir* **2002**, *18*, 3441.
- (12) Adachi, E.; Dimitrov, A. S.; Nagayama, K. *Langmuir* **1995**, *11*, 1057.
- (13) Pieranski, P.; Stezleski, L.; Pansu, B. *Phys. Rev. Lett.* **1983**, *50*, 90.
- (14) Cong, H.; Cao, W. *Langmuir* **2003**, *19*, 8177.
- (15) Hadjiiski, A.; Dimova, R.; Denkov, N. D.; Ivanov, I. B.; Borwankar, R. *Langmuir* **1996**, *12*, 6665.
- (16) Wang, H.; Li, X.; Nakamura, H.; Miyazaki, M.; Maeda, H. *Adv. Mater.* **2002**, *14*, 1662.

JA0497750